

The Progenitor of SN 2005cs in the Whirlpool Galaxy

Justyn R. Maund¹, Stephen J. Smartt² and I. John Danziger³

¹*Institute of Astronomy, University of Cambridge, Madingley Road, Cambridge CB3 0HA, England, UK*

²*Department of Physics and Astronomy, Queen's University, Belfast BT7 1NN, Northern Ireland, UK*

³*Osservatorio Astronomico di Trieste, INAF, Via Tiepolo 11 34131 Trieste, Italia*

27 August 2018

ABSTRACT

The progenitor of SN 2005cs, in the galaxy M51, is identified in pre-explosion HST ACS WFC imaging. Differential astrometry, with post-explosion ACS HRC F555W images, permitted the identification of the progenitor with an accuracy of $0.006''$. The progenitor was detected in the F814W pre-explosion image with $I = 23.3 \pm 0.2$, but was below the detection thresholds of the F435W and F555W images, with $B < 24.8$ and $V < 25$ at 5σ . Limits were also placed on the U and R band fluxes of the progenitor from pre-explosion HST WFPC2 F336W and F675W images. Deep images in the infra-red from NIRI on the Gemini-North telescope were taken 2 months prior to explosion, but the progenitor is not clearly detected on these. The upper limits for the JHK magnitudes of the progenitor were $J < 21.9$, $H < 21.1$ and $K < 20.7$. Despite having a detection in only one band, a restrictive spectral energy distribution of the progenitor star can be constructed and a robust case is made that the progenitor was a red supergiant with spectral type between mid-K to late-M. The spectral energy distribution allows a region in the theoretical HR diagram to be determined which must contain the progenitor star. The initial mass of the star is constrained to be $M_{ZAMS} = 9_{-2}^{+3}M_{\odot}$, which is very similar to the identified progenitor of the type II-P SN 2003gd, and also consistent with upper mass limits placed on five other similar SNe. The upper limit in the deep K-band image is significant in that it allows us to rule out the possibility that the progenitor was a significantly higher mass object enshrouded in a dust cocoon before core-collapse. This is further evidence that the trend for type II-P SNe to arise in low to moderate mass red supergiants is real.

Key words: stellar evolution: general – supernovae:general – supernovae:individual:2005cs – galaxies:individual:M51

1 INTRODUCTION

Stellar evolution models predict that stars with initial masses $> 8M_{\odot}$ end their lives in a core-collapse induced supernova (CCSN), and the CCSN mechanism is also related to the energetic gamma-ray burst (GRB) phenomenon (Matheson et al. 2003). The study of the progenitors of CCSNe is essential to both the understanding of the evolution of SNe and the massive stars which produce them. Fortuitous pre-explosion observations of the progenitor can allow the determination of the evolutionary state of the star prior to SN explosion. The progenitor of SN 1987A was found to be a blue supergiant (Walborn et al. 1989), whereas the progenitor of SN 1993J was identified as a red supergiant with a UV excess due to a hot binary companion (Aldering et al. 1994; Maund et al. 2004). In the cases of SNe 1987A and 1993J the direct observations of the progenitors have helped explain peculiarities in the SN explosions themselves. The progenitor of the type II-P SN 2003gd was identified as a red supergiant, the canonical prediction of stellar evolution models for this type of SN (Smartt et al. 2004; Van Dyk et al. 2003b). Li et al. (2005a) report the identification of a yellow super-

giant progenitor for the type II-P SN 2004et. Recently Maund et al. (2005) and Maund & Smartt (2005) have placed limits on CC-SNe, of various types, whose progenitors were not detected on pre-explosion imaging. Maund & Smartt (2005) demonstrate the importance of high resolution post-explosion imaging of SNe, using differential astrometry to locate (with sub-pixel accuracy) the progenitor on pre-explosion images.

In this letter we report the identification of the progenitor of the Type II-P SN 2005cs in M51, the “Whirlpool Galaxy.” SN 2005cs was discovered by Kloehr (2005) on 2005 June 28.9. The SN was spectroscopically classified as a Type II by Modjaz et al. (2005), with P-Cygni profiles of the Balmer and He lines. Richmond (2005) and Li et al. (2005b) reported the identification of two different stars as possible progenitors for this object: a blue and a red star respectively. Li et al. (2005b) give the position of SN 2005cs as $\alpha_{2000} = 13^{\text{h}}29^{\text{m}}52.^{\text{s}}76$, $\delta_{2000} = 47^{\circ}10'36.''11$. This implies an offset between SN 2005cs and the centre of M51 of $\Delta\alpha = 6''$ and $\Delta\delta = -64.7''$, or 2.7kpc at a distance of 8.4Mpc (Feldmeier et al. 1997, with P.A. and inclination of M51 as quoted

Table 1. Pre-and post-explosion observations of the site of SN 2005cs used in this paper.

Date	Instrument	Filter	Exp. Time (s)
Pre-explosion images			
2005 Jan 20-21	ACS/WFC	F435W	2720
	ACS/WFC	F555W	1360
	ACS/WFC	F814W	1360
1999 Jul 21	WFPC2	F336W	1200
	WFPC2	F555W	1200
	WFPC2	F675W	500
2005 Apr 29	NIRI	<i>J</i> (G0202)	500
	NIRI	<i>H</i> (G0203)	500
	NIRI	<i>K</i> (G0204)	625
Post-explosion images			
2005 Jul 24	ACS/HRC	F555W	80/160/1704

by HyperLEDA¹ as 163° and 47.5° respectively). While this paper was in the process of submission, a similar study was submitted for publication by Li et al. (2005c). There are some differences in the results of the two studies and we briefly highlight them in this letter where appropriate.

2 OBSERVATIONS AND DATA REDUCTION

The pre- and post-explosion images analysed here are summarised in Table 1. Pre-explosion images of the site of SN 2005cs were available in the Hubble Space Telescope (HST) archive², with multi-colour imaging with the Wide Field Planetary Camera 2 (WFPC2) and Advanced Camera for Surveys (ACS) Wide Field Channel (WFC). Individual HST WFPC2 observations were retrieved from the STScI archive. These observations were calibrated with the On-the-fly-recalibration (OTFR) pipeline. The site of SN 2005cs was located on the WF2 chip in the 1999 WFPC2 observations, which has $0.1'' \text{ pix}^{-1}$. The WFPC2 observations were combined for the extraction of cosmic rays and corrected for geometric distortions. Aperture photometry was then conducted on these images using DAOPHOT. PSF photometry was conducted on the WFPC2 observations using the HSTPHOT package (Dolphin 2000). HSTPHOT includes corrections for chip-to-chip variations, charge transfer efficiency and transformations from the WFPC2 photometric system to the standard Johnson-Cousins magnitude system. The WFPC2 pre-explosion observation complemented the ACS pre-explosion imaging with observations in F336W and F675W (approximately U and R respectively).

The ACS pre-explosion images were acquired as part of program GO-10452 (PI: S.V.W. Beckwith), which conducted a large deep mosaic of M51 (NGC 5194) and its companion NGC 5195. These observations were in four bands F435W, F555W, F814W and F658N. The drizzled combined mosaic frames were available from STScI (Mutchler et al. 2005), with scale $0.05'' \text{ pix}^{-1}$. Aperture and PSF photometry was conducted on the mosaic frames using the PYRAF implementation of the DAOPHOT algorithm. Empirical

aperture corrections were applied to the data, with the charge transfer efficiency corrections of Riess & Mack (2004) and the colour transformation equations and updated zeropoints of Sirianni et al. (2005).

Infrared pre-explosion observations of the site of SN 2005cs were conducted with the Gemini North Telescope Near Infrared Imager (NIRI) in the *JHK* bands. These observations were conducted as part of program GN-2005A-Q-49 (PI: S. Smartt). The *f/6* camera of NIRI was used to provide imaging with scale $0.117'' \text{ pix}^{-1}$. The observations were split into a series of short sub-exposures, to overcome the sky background, with small offsets between each sub-exposure. On completion of the series of observations on target, a comparable series of short exposures at a large offset was immediately acquired to measure the levels of the IR sky background. The NIRI images were reduced and combined, with sky subtraction, using the IRAF *gemini* package of reduction tools for the NIRI instrument. Photometry on the *JHK* images was done by PSF fitting within the IRAF implementation of DAOPHOT. The zero-point of the NIR filters was determined using two standard stars (UKIRT Faint Standards 133 and 136) taken before and after the science frames. They gave comparable results, and suggested that the period of the observations was stable and photometric. The image quality was $0.5''$ in *K* and $0.6''$ in *J* and *H*.

Post-explosion ACS High Resolution Channel (HRC) imaging was conducted as part of program GO-10498 (PI: S. Smartt). These observations were only acquired in the F555W, as good colour information on the surrounding stellar population was possible from the pre-explosion observations. These were photometered in a similar way to the pre-explosion ACS/WFC observation using PYRAF DAOPHOT. The same corrections were applied, although the magnitudes were left in the ACS VegaMag photometric system.

The geometric transformation between the F555W images of WFPC2 1999 observations with 2005 ACS/WFC observations was calculated, using the IRAF task *geomap*, with 11 common stars. X- and Y- offsets between the F555W image and other filter images from the same observing run were calculated by cross-correlating the images, using the STSDAS *crossdriz* task with the offset calculated from the cross correlation image using *shiftfind*. The geometric transformation was also calculated between the 2005 ACS/WFC F814W image and the NIRI *J*-band image, with the shift calculated between the ACS/WFC F555W and F814W images applied to bring the transformed NIRI *J*-band image to the same coordinate system as the ACS/WFC F555W image. Similarly to the HST pre-explosion observations, offsets between the *J*-band image and the *H* and *K* images were calculated using the cross correlation method. The uncertainty in transforming the position of a star from one image to another was calculated as the sum in quadrature of the positional uncertainties in the reference image and transformed image and the r.m.s. uncertainty of the transformation, by *geomap*. The position uncertainties on the individual images were assessed by measuring the scatter in the positions of the stars, measured using the four centering algorithms of DAOPHOT, of all the stars used to calculate the geometric transformation. The individual image position uncertainty was taken as the sum in quadrature of the mean scatter and standard deviation about this mean in both the X and Y directions.

3 OBSERVATIONAL RESULTS

SN 2005cs was detected in the post-explosion ACS/HRC F555W imaging with $m_{F555W} = 15.28 \pm 0.01$. The position of SN 2005cs

¹ <http://www-obs.univ-lyon1.fr/hypercat/>

² <http://archive.stsci.edu/hst/>

on the post-explosion frame was calculated to within $\pm 0.002''$. The position of the SN on pre- and post-explosion images is shown on Fig. 1. The SN position on the pre-explosion ACS/WFC F555W image was identified to within $0.006''$ (which is the combined uncertainties on the determination of positions on the pre- and post-explosion images and the geometric transformation). A progenitor star is significantly detected on the F814W image with $m_{F814W} = 23.26 \pm 0.03$. There is no object in the pre-explosion F435W and F555W images, and we estimate 5σ detection limits of $m_{F435W} = 24.9$ and $m_{F555W} = 25$ (using the methods of Maund & Smartt 2005). In order to add further limits to the spectral energy distribution (SED) of the progenitor, we determined the limiting magnitude of the WFPC2 F336W and F675W images. Due to the lower resolution of these images compared to the ACS, the progenitor position was too close to the brighter object to the southwest to allow accurate simultaneous PSF fitting. Hence a large (6 pixel) aperture flux was determined at the progenitor position, and the flux of stars which had well determined individual small aperture photometry was subtracted. This suggested there was no residual flux from any object brighter than $m_{F336W} = 21.1$ and $m_{F675W} = 23.6$. Li et al. (2005c) report a magnitude of $I = 24.15 \pm 0.20$ for the progenitor which is significantly fainter than our measurement. We have extensively checked our ACS photometry and zeropoints using several methods (e.g. DOLphot³ and several alternative experiments with PSF and aperture photometry) and also compared the F814W magnitudes (from HSTphot and our own estimates) of faint isolated stars in WFPC2 archive images with our ACS measured magnitudes. We find no problems or inconsistencies in our analysis and confirm the magnitude as $m_{F814W} = 23.26 \pm 0.03$.

The location of the SN on the pre-explosion Gemini NIRI imaging was identified to within $0.078''$. There is a *JHK* source clearly detected close to the position of the *I*-band progenitor, however its position is more than 2σ away and hence is not spatially coincident with the progenitor. This object has also been detected by Li et al. (2005c) in NICMOS pre-explosion images, and is coincident with the *I*-band star to the north west of the progenitor. At the position of the progenitor in the *JHK* NIRI images, the flux does appear somewhat higher than the surrounding background, but given the ground-based resolution there is no evidence for detection of a single source (see Fig. 1). A further check was performed to determine that no object could be detected in the *K*-band. The bright objects on the image were subtracted off by PSF fitting, and fainter objects were identified on the resultant frame. After three iterations of PSF fitting and subtraction, a boxcar median filtered image was constructed, which should be representative of the varying galaxy background. This was subtracted off the original frame and the photometric procedure was repeated. There was no evidence of a single point source at the progenitor position. The detection limits in the *JHK*-band images were determined at the SN position. In the first instance statistical calculations of the 3σ detection limits were determined from the detector characteristics and the sky noise. This was compared with the measured magnitudes of the faintest real objects in the images which could be visually identified and which were both well fit with a PSF and subtracted off cleanly. The 3σ calculated limits were significantly fainter (by ~ 0.7 mag) than these objects, but the 5σ limits agreed well with the magnitudes of the faintest sources measured in the image. Hence we adopted the 5σ limits, which are: $J = 21.9$, $H = 21.1$ and $K = 20.7$. The *JH*

limits are consistent with the NICMOS limits reported by Li et al. (2005c), although the additional *K*-band upper limit we present has significant implications (see Section 4.3).

4 DISCUSSION

4.1 Estimates of metallicity of the progenitor region

HII regions around M51 were spectroscopically studied by Bresolin et al. (2004) for the purposes of abundance analysis. The sight line corrected angular distance of SN 2005cs is $66.5''$ or $0.21R_0$ (where R_0 is the characteristic radius which Bresolin et al. (2004) give as $5.4'$). The oxygen abundance, at the radius of SN 2005cs, was calculated to be $12 + \log(O/H) = 8.66 \pm 0.11$, which is similar to abundance in the HII region CCM 56 (> 8.58 dex) closest to SN 2005cs. Bresolin et al. (2004) point out that their new abundance determinations, which are based on directly determined electron temperatures, are significantly lower than previous estimates in M51 and that the previously reported very metal rich abundances are likely to have been inaccurate. As Asplund et al. (2004) give the solar oxygen abundance as 8.66 ± 0.05 , this implies that the metallicity appropriate for SN 2005cs and its progenitor star is very likely to be in the range $1 \pm 0.3Z_{\odot}$.

4.2 Estimates of Reddening

Modjaz et al. (2005) reported the presence of Galactic and host galaxy components of the NaID lines in an early spectrum of SN 2005cs. They reported that the equivalent width of the host-galaxy component was similar in strength to the Galactic component of 0.2\AA . Turatto et al. (2003) provide relationships between the strength of the NaID absorption and the reddening from the intervening medium. If one assumes that the strengths of the two NaID components may be added then the total NaID line strength implies a reddening between $E(B - V) = 0.05 - 0.16$. Bresolin et al. (2004) record the reddening coefficient $c(H\beta)$ for the nearby HII region CCM 56 of 0.23 which corresponds to $E(B - V) = 0.16$ with a Galactic Howarth (1983) reddening law. The three colour photometry of red supergiants ($B - V > 0.2$) within $2''$ of SN 2005cs was also used to estimate the reddening as detailed in Maund & Smartt (2005). Stellar positions were plotted on a two-colour diagram ($B - V$ vs. $V - I$) and compared with a theoretical supergiant colour sequence. The weighted mean displacement of the stars' positions, along the reddening vector, from the theoretical colour sequence provided a measure of reddening. This technique yielded a value of $E(B - V) = 0.12 \pm 0.01$, and we hence adopt a reddening of $E(B - V) = 0.14 \pm 0.02$ throughout the rest of this paper.

4.3 The Progenitor of SN 2005cs

There is a clear and unambiguous detection of the progenitor of SN2005cs in the ACS F814W image. As we have only one detection, the colour of the star makes the transformation from the F814W to standard Johnson *I* a little uncertain, and indeed all the transformations between the ACS filters and standard *BVRI* are subject to a similar uncertainty. However from the non-detections in the other bands, we can confidently say that it was a red star, later than mid K-type and the corrections between the ACS and Johnson *VRI* system are at most 0.2 mag, if the star was at the extreme

³ <http://purcell.as.arizona.edu/dolphot/>

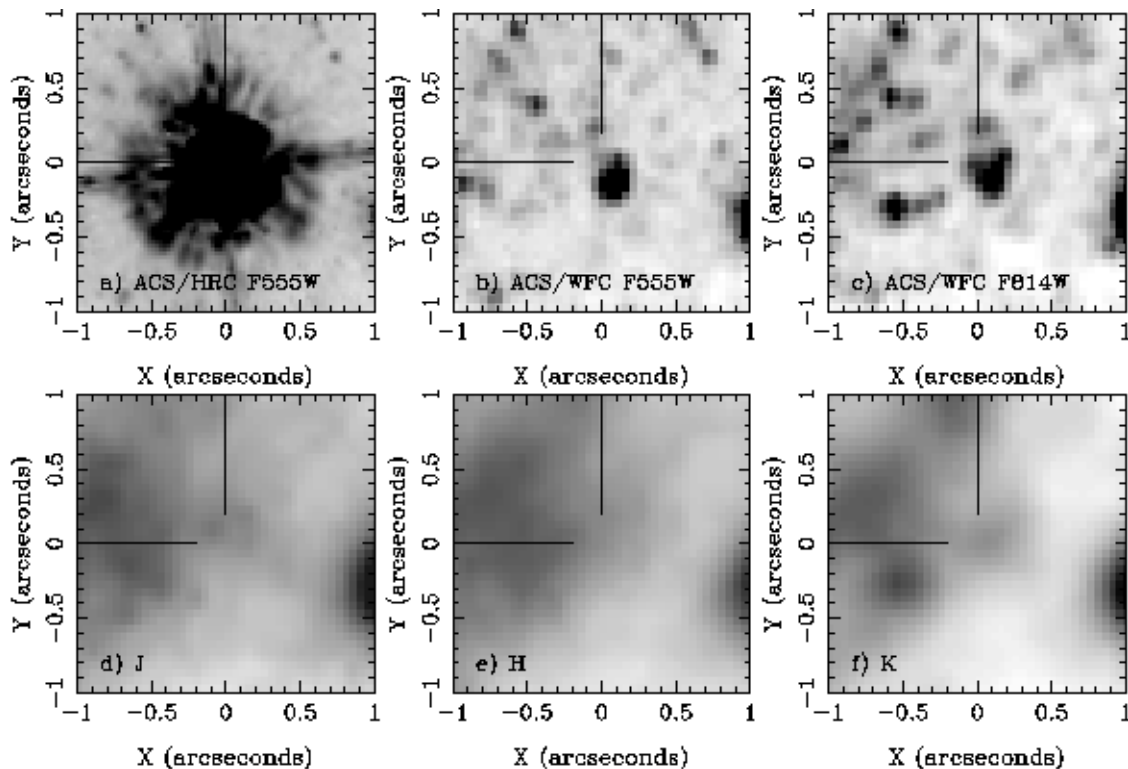


Figure 1. Pre- and post-explosion images of the site of SN 2005cs in M51. a) Post-explosion ACS/HRC F555W image (160 s) of SN 2005cs, the cross hairs indicate the centre of the PSF. The observation was split into short exposures to avoid saturation of the SN centroid. b) Pre-explosion ACS/WFC F555W image, in which the progenitor is not detected to $m_{F555W} = 25$ at 5σ . c) Pre-explosion ACS/WFC F814W image, the progenitor is detected in this image, indicated by the cross hairs, with $m_{F814W} = 23.26$. d) Pre-explosion NIRI *J*-band image. e) Pre-explosion NIRI *H*-band image. f) Pre-explosion NIRI *K*-band image. The images are aligned to the reference ACS/WFC F555W image (panel b), such that North is up and East is left.

M5 cool end (Maud & Smartt 2005). Hence in the rest of this discussion we interpret the ACS filter magnitudes as standard *BVRI*, and the relatively small uncertainties are included in the error analysis. The non-detection of a source in the *BVR*-band images is a very robust argument that the star was red. The spectral energy distribution of the progenitor star in *BVRIJHK* is shown in Fig. 2. This is consistent with a red supergiant which is between K5 and M5. The star cannot have had bluer colours than a mid K-type, or it would have been detected in the *VR*-bands.

Although there is a range in possible spectral types that would fit the stellar SED, we can still set restrictive luminosity and mass limits on the red progenitor star. Using the standard reddening law of Cardelli et al. (1989), it has a $(V - I)_0 > 1.52$, which corresponds to a supergiant redder than approximately K3 (Elias et al. 1985). The effective temperatures of red supergiants, $(V - I)_0$ colours and bolometric corrections from Elias et al. (1985) and also Drilling & Landolt (2000) can then be used to determine a location box in the theoretical HR-diagram. This is shown in Fig. 3, with the stellar evolution tracks from the Geneva group plotted at $Z = Z_\odot$ (Meynet et al. 1994). The range in $\log L$ at a constant T_{eff} comes from the quadrature combined errors in distance, reddening, measured *I*-band magnitude (including colour correction), and bolometric correction (assuming plus or minus one spectral subtype). We can place quite a restrictive box on the location of the red supergiant progenitor in the HRD, even with a detection in only one band. The star was likely to have been a red supergiant of initial mass $9_{-2}^{+3}M_\odot$. Li et al. (2005c) report an initial mass of $7 - 9M_\odot$, and indeed the position of the progenitor is closer to $7M_\odot$ in their

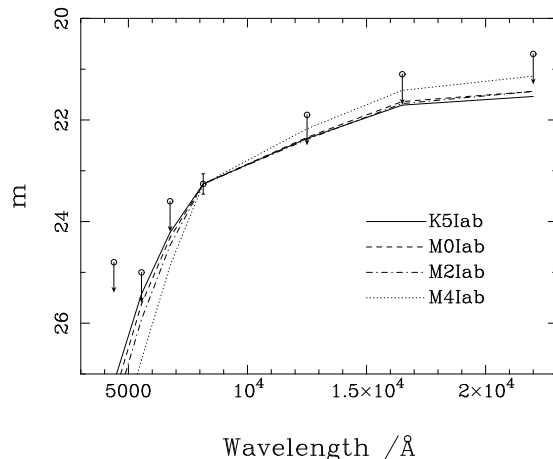


Figure 2. The spectral energy distribution of the progenitor is constrained by the *I*-band detection, and the upper limits in *VRJHK*. The star cannot have been bluer than a mid K-type, or it would have been detected in the *V* and *R* bands. The colours of the K5Ia-M4Iab Galactic supergiants were taken from Elias et al. (1985), and scaled to $I=23.26$ with appropriate reddening as discussed in the text.

figure. The difference of 1 magnitude in the *I*-band is responsible for the higher mass that we report, although within the errors the two studies are in agreement. This is a very similar mass to that derived for the progenitor of SN 2003gd, which was also a red supergiant of initial mass $8_{-2}^{+4}M_\odot$ (Smartt et al. 2004). Both

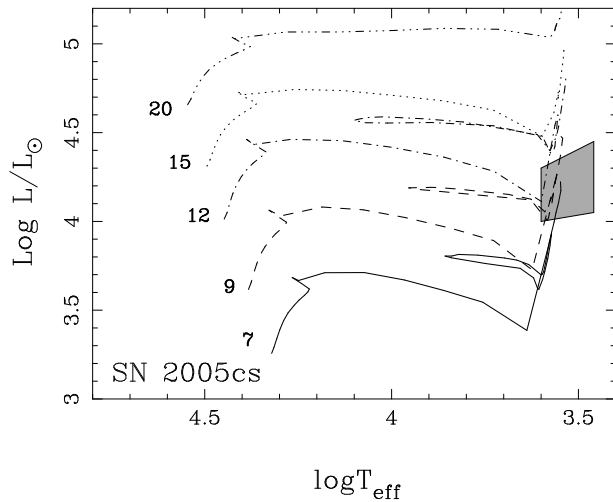


Figure 3. The position of the progenitor of SN2005cs is restricted to lie in the grey shaded region. The evolutionary tracks are the non-rotating models from the Geneva group (Meynet et al. 1994), where the initial mass, in units of M_{\odot} , is indicated for each track. The cool limit of the allowed region is the lowest observed T_{eff} of late M-type supergiants.

these supernovae were of type II-P (Li et al. 2005c; Hendry et al. 2005) and future comparison of the photometric and spectral evolution of SN 2005cs will determine how similar they actually are. As pointed out by Smartt et al. (2004) and Li et al. (2005c), there is growing evidence that SNe II-P tend to arise in red supergiants with masses lower than $\sim 15M_{\odot}$. There are restrictive mass limits, or detections, now set for seven SNe II-P (SNe 1999br, 1999em, 1999gi, 2001du, 2003gd, 2004et, 2005cs) and none of them are higher than $15M_{\odot}$ (Maund & Smartt 2005; Smartt et al. 2003; Li et al. 2005a; Van Dyk et al. 2003a,b). One possibility often suggested to explain this is that the progenitors may be dust enshrouded red supergiants and hence appear to have lower mass and lower luminosity. Although the SNe themselves are not reddened, a plausible scenario is the destruction of this dust by the explosion (Graham & Meikle 1986). However the deep K -band image argues against this scenario. Even if the visual extinction were as high as $A_V = 5$, the K -band images would be sensitive to stars with $M_K < -9.5$, and with the bolometric corrections of Elias et al. (1985) this implies $\log L/L_{\odot} < 4.6$. Even when conservative errors on the distance, limiting magnitudes and bolometric correction are included (resulting in ± 0.2 dex), Fig. 3 shows that this rules out red supergiants with masses greater than $12M_{\odot}$.

In summary, this letter presents the unambiguous detection of a red supergiant as the progenitor of SN 2005cs. We show that the likely initial mass for the star was in the range $M_{ZAMS} = 9^{+3}_{-2}M_{\odot}$. This adds to the emerging argument that all type II-P supernovae lie in the low to moderate mass range of red supergiants. The upper limit from the deep K -band image is evidence that these are not dust enshrouded higher mass objects that have their cocoons destroyed in the explosion.

ACKNOWLEDGMENTS

Based on observations made with the NASA/ESA Hubble Space Telescope, and on observations with the Gemini Observatory, which is operated by the Association of Universities for Research in Astronomy, Inc., under a cooperative agreement with the NSF

on behalf of the Gemini partnership. JRM and SJS acknowledge financial support from PPARC. We thank the referee, S. Ryder, for his useful comments and discussion.

References

- Aldering G., Humphreys R. M., Richmond M., 1994, *AJ*, 107, 662
 Asplund M., Grevesse N., Sauval A. J., Allende Prieto C., Kiselman D., 2004, *A&A*, 417, 751
 Bresolin F., Garnett D. R., Kennicutt R. C., 2004, *ApJ*, 615, 228
 Cardelli J. A., Clayton G. C., Mathis J. S., 1989, *ApJ*, 345, 245
 Dolphin A. E., 2000, *PASP*, 112, 1383
 Drilling J. S., Landolt A. U., 2000, in Cox A. N., ed., *Allen's Astrophysical Quantities*, p381, 4 edn, AIP, New York
 Elias J. H., Frogel J. A., Humphreys R. M., 1985, *ApJS*, 57, 91
 Feldmeier J. J., Ciardullo R., Jacoby G. H., 1997, *ApJ*, 479, 231
 Graham J. R., Meikle W. P. S., 1986, *MNRAS*, 221, 789
 Hendry M. A., Smartt S. J., Maund J. R., Pastorello A., Zampieri L., Benetti S., Turatto M., et al. 2005, *MNRAS*, 359, 906
 Howarth I. D., 1983, *MNRAS*, 203, 301
 Kloehr W., 2005, *IAUC*, 8553
 Li W., Van Dyk S. D., Filippenko A. V., Cuillandre J., 2005a, *PASP*, 117, 121
 Li, W. Van Dyk S.D. Filippenko A.V. and Cuillandre J.-C. 2005b, *IAUC*, 8556
 Li W., Van Dyk S. D., Filippenko A. V., Cuillandre J., Jha S., Bloom J. S., Riess A. G., Livio M., 2005c, *ArXiv Astrophysics e-prints* 0507394
 Matheson T., Garnavich P. M., Stanek K. Z., Bersier D., Holland S. T., Krisciunas K., Caldwell N., Berlind P., et al. 2003, *ApJ*, 599, 394
 Maund J. R., Smartt S., Schweizer F., 2005, *ArXiv Astrophysics e-prints* 0506436
 Maund J. R., Smartt S. J., 2005, *MNRAS*, 360, 288
 Maund J. R., Smartt S. J., Kudritzki R. P., Podsiadlowski P., Gilmore G. F., 2004, *Nature*, 427, 129
 Meynet G., Maeder A., Schaller G., Schaerer D., Charbonnel C., 1994, *A&A Suppl.*, 103, 97
 Modjaz M., Kirshner R., Challis P., Hutchins R., 2005, *IAUC*, 8555
 Mutchler M., Beckwith S. V. W., Bond H.E., Christian C., Frattare L., Hamilton F., Hamilton M., Levay Z., et al., 2005, *BAAS*, 37, 2
 Richmond M. W., 2005, *IAUC*, 8555
 Riess A., Mack J., 2004, *Instrument Science Report ACS 2004-006*, Time Dependence of ACS WFC CTE Corrections for Photometry and Future Predictions. Space Telescope Science Institute
 Sirianni M., Jee M. J., Benítez N., et al., 2005, *PASP*, in press, *ArXiv Astrophysics e-prints* 0507614
 Smartt S. J., Maund J. R., Gilmore G. F., Tout C. A., Kilkenny D., Benetti S., 2003, *MNRAS*, 343, 735
 Smartt S. J., Maund J. R., Hendry M. A., Tout C. A., Gilmore G. F., Mattila S., Benn C. R., 2004, *Science*, 303, 499
 Turatto M., Benetti S., Cappellaro E., 2003, in *From Twilight to Highlight: The Physics of Supernovae Variety in Supernovae*. pp 200, ESO Garching
 Van Dyk S. D., Li W., Filippenko A. V., 2003a, *PASP*, 115, 448
 Van Dyk S. D., Li W., Filippenko A. V., 2003b, *PASP*, 115, 1289
 Walborn N. R., Prevot M. L., Prevot L., Wamsteker W., Gonzalez R., Gilmozzi R., Fitzpatrick E. L., 1989, *A&A*, 219, 229